23

Modeling of optical-acoustic detectors with cylindrical resonators of variable cross-section

© A.V. Borisov, D.R. Makashev, A.A. Boyko, Yu.V. Kistenev

National Research Tomsk State University,
Tomsk, Russia

e-mail: yv.kistenev@gmail.com

Received August 05, 2025
Revised August 25, 2025
Accepted November 25, 2025

The results of a numerical study of the characteristics of a resonant optical-acoustic detector (OAD) with two coupled cylindrical resonators of variable cross-section using a dynamic model are presented. The dependences of the pressure amplitude in the center of the resonator (where the antinode of the standing acoustic wave is located) are obtained, and it is shown that an increase in the resonator cross-section in the region of the antinode of the acoustic wave relative to their initial cross-section leads to an increase in pressure in this region, which can be used to increase the sensitivity of the OAD. It is also shown that the sensitivity estimates obtained using the widely used analytical formula for calculating the sensitivity of resonant OAD are fundamentally different from the results of calculations of the dynamic model for OAD with resonators of variable cross-section. This indicates that the analytical expression is inapplicable for assessing the sensitivity of resonant OADs with resonators of variable cross-section.

Keywords: optical-acoustic detector, cylindrical resonator of variable cross-section.

DOI: 10.61011/EOS.2025.12.63183.40-25

Introduction

Registering the profile of the volatile molecular markers in exhaled air is considered a promising method of conducting medical screening tests [1,2]. This method is easy to use, comfortable for the patient, and the results show its effectiveness in diagnosing bronchopulmonary, oncological diseases, diabetes, and myocardial infarction [3–8]. There are three main groups of instrumental methods for detecting volatile molecular markers in exhaled air: gas chromatography, chemical sensors (electronic nose), and gas absorption spectroscopy [8]. The latter is most suitable for routine clinical measurements in terms of a combination of parameters such as selectivity, sensitivity, stability of characteristics, and when there's a lack of consumables. Since the concentration of most of these markers is low (at the level of ppm and ppb units), it is critically important to increase the sensitivity of instrumental methods.

Laser optical-acoustic spectroscopy is one of the most sensitive methods of the absorption gas analysis [9,10]. The principle of this method is based on the absorption of pulsed or modulated laser radiation by the test mixture located in the measuring cell, while the absorbed energy is converted into heat, creating an acoustic wave with a frequency equal to the frequency of laser radiation modulation. The acoustic wave exerts periodic pressure on the walls of the measuring cell, which is registered by the microphone. Sensitivity of the optical-acoustic spectrometers depends on design of optical-acoustic detector (OAD). Resonant OADs based on the use of acoustic resonance have the highest sensitivity [11]. When the modulation frequency of the laser radiation coincides with the frequency of the acoustic resonance of the measuring cell, the signal on the microphone rises proportionally to the quality of the acoustic resonance. The value of the latter can reach several hundreds.

Resonant OADs using Helmholtz differential resonators jcite12,13 consist of two identical cylindrical resonators arranged in parallel, the open ends of which are connected in pairs by buffer elements. A microphone is installed in each of the resonators (Fig. 1, *a*). Fig. 1, *b* shows the pressure wave profile in the horizontal section of the OAD for the first four resonant modes, where in the first mode the maximum and minimum pressures are located in the resonators' center. A similar situation is realized for the fourth mode, but in this case the resonant frequency is significantly higher. For the second and third modes, the pressure maxima and minima are located not in resonators, but in buffers, and the difference between the maximum and minimum pressures in these cases is significantly less than in the case of the first and fourth modes. The first resonant mode is of the greatest practical interest, since it corresponds to a lower frequency for all modes, and it is possible to use a differential detection mode if two acoustic microphones are located in the center of the resonators. At the same time, subtracting electrical signals from the microphones allows doubling the effective signal and significantly suppressing any noise. This OAD design is widely used in optical-acoustic spectrometers [14–19].

The sensitivity of the cylindrical OAD is determined by microphone sensitivity and the amplitude of the pressure

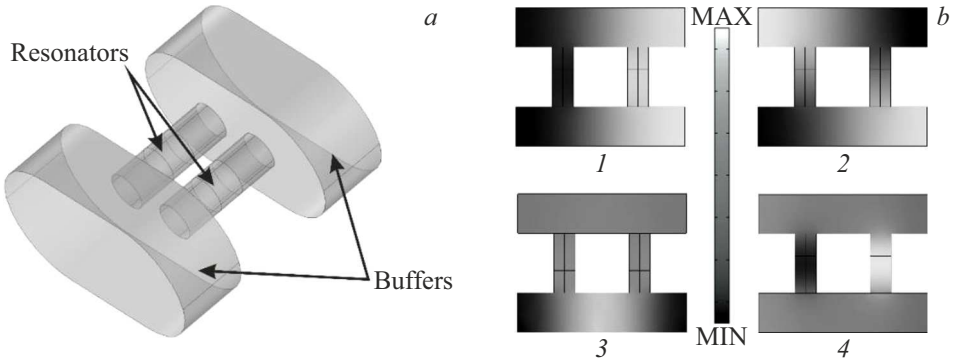

Figure 1. Layout of OAD with two constant radius cylindrical resonators (a) and profile of the pressure wave in horizontal section of OAD for the first (digits *1–4*) resonance modes (b).

wave, which is found from the expression [20]

$$A_n(\omega_n) = \frac{(y-1)LQ_nF_n}{V_{\text{cell}}\omega_n}\alpha W_L, \qquad (1)$$

where $A_n(\omega_n)$ — amplitude of pressure „surge“ γ — adiabatic index L —length of the measurement cell, Q_n — Q factor of the cell on harmonic with number n, V_{cell} — cell volume, ω_n — frequency of harmonic n, F_n — normalized overlapping integral for the harmonic n, α — medium absorption coefficient, W_L — laser radiation power.

Since sensitivity of OAD is proportional to the power of the laser radiation sent to the cell, optical parametric oscillators with a power of tens of mW are often used as radiation sources [14]. However, they are quite bulky and have a wide generation line (of the order of $1-3\,\text{cm}^{-1}$). Diode and quantum cascade lasers are compact and have a narrow generation line, but their power is several orders of magnitude lower. Partially, the latter disadvantage can be compensated by optimizing the design of OAD.

Computational modelling is widely used to find optimal characteristics of OAD with cylindrical resonators [21–28]. Optimization is aimed at finding the geometric parameters of resonators and buffers that ensure high Q-factor of the OAD and sensitivity of the spectrometer. The shape of the resonator may serve as an additional improvement of the spectrometer characteristics.

The purpose of this work is to numerically study the acoustic properties of OAD with two coupled cylindrical resonators of variable cross-section.

Materials and methods

In this paper, a resonant OAD with two cylindrical resonators of variable cross section is reviewed (Fig. 2). In the first option (Fig. 2, a) cylindrical resonators are used with their cross-section radius having two local minima which are smaller than the cross-section radius at the junction of buffer elements and resonators. In the second option (Fig. 2, b) cylindrical resonators are used where the cross-section radius is minimal at the buffers-resonators junction and grows monotonously towards the center of each of the resonators. In both variants, the cross-section radius is maximal in the center of each of the resonators.

In modeling, a resonant OAD with resonators of constant cross-section with a Q factor of 556 was used as a basis [21]. Its geometrical parameters: $D = 60\,\text{mm}$, $L = 47.5\,\text{mm}$, $r = 8.5\,\text{mm}$, $R = 29\,\text{mm}$, $l = 31.5\,\text{mm}$.

For OAD shown in Fig. 2 the following system of equations was solved:

$$\frac{\partial\tilde{\rho}}{\partial t} + \nabla(\tilde{\rho}\mathbf{v}) = 0, \qquad (2)$$

$$\tilde{\rho}\left(\frac{\partial\mathbf{v}}{\partial t} + (\mathbf{v}\cdot\nabla)\mathbf{v}\right) = -\nabla\tilde{p} + \mu\nabla^2\mathbf{v} + \left(\xi + \frac{\mu}{3}\right)\nabla(\nabla\cdot\mathbf{v}), \qquad (3)$$

$$\nabla\rho C_p\left(\frac{\partial\tilde{T}}{\partial t} + \mathbf{v}\cdot\nabla\tilde{T}\right) = \nabla\cdot(k\nabla\tilde{T}) + \alpha\tilde{T}\frac{\partial\tilde{p}}{\partial t} + Q, \qquad (4)$$

$$\tilde{\rho}C_p\left(\frac{\partial\tilde{T}}{\partial t} + \mathbf{v}\cdot\nabla\tilde{T}\right) = \nabla\cdot(k\nabla\tilde{T}) + \alpha\tilde{T}\frac{\partial\tilde{p}}{\partial t} + Q, \qquad (4)$$

$$\tilde{p} = \tilde{\rho}RT. \qquad (5)$$

Here $\tilde{\rho}$ — density, $\mathbf{v}$ — velocity, $\tilde{p}$ — pressure, $\tilde{T}$ — temperature, t — time, μ — dynamic viscosity, ξ — volumetric viscosity, C_p — constant pressure heat capacity, k — thermal conductivity coefficient, α — thermal expansion coefficient, Q — external thermal energy, R — universal gas constant, ∇ — nabla operator, the dot notation means a scalar product. The studied gas mixture was considered to be an ideal gas.

In case of small deviations from the equilibrium values($\tilde{\rho} = \rho_0 + \rho$, $\rho \ll \rho_0$, $\tilde{T} = T_0 + T$, $T \ll T_0$, $\tilde{p} = p_0 + p$, $p \ll p_0$) the system (2)–(5) may be rewritten as follows:

$$\frac{\partial\rho}{\partial t} + \rho_0\nabla\cdot\mathbf{v} = 0, \qquad (6)$$

$$\rho_0\frac{\partial v}{\partial t} = -\nabla p + \mu\nabla^2\mathbf{v}, \qquad (7)$$

$$\rho C_p\frac{\partial T}{\partial t} = k\nabla^2 T + \alpha T_0\frac{\partial p}{\partial t} + Q, \qquad (8)$$

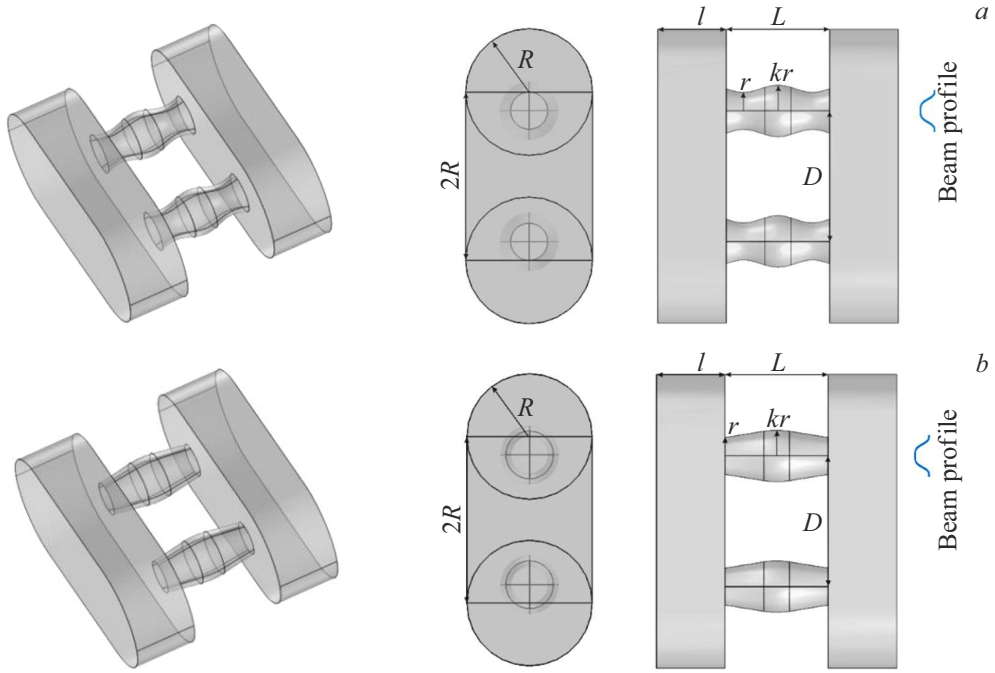

Figure 2. OAD with two cylindrical resonators of variable radius for geometric shapes (a) of the first and (b) second types. r — minimum resonator radius, $k > 1$ — coefficient characterizing maximum resonator radius, D — distance between resonators, L — length resonators, R — radii of the corresponding buffer elements, l — length of buffers.

$$p = c^2\rho + \alpha\gamma\rho_0 T. \tag{9}$$

Here γ — adiabatic index, $c = \sqrt{\gamma RT_0}$ — sound velocity.

For the harmonic waves $\rho = \varrho e^{i\omega t}$, $p = Pe^{i\omega t}$, $\mathbf{v} = \mathbf{u}e^{i\omega t}$ (it was taken into account that the equilibrium velocity was zero), $T = \Theta e^{i\omega t}$ system (6)–(9) will be written as

$$i\omega\varrho + \rho_0\nabla\cdot\mathbf{u} = 0, \tag{10}$$

$$i\omega\rho_0 u = -\nabla P + \mu\nabla^2\mathbf{u}, \tag{11}$$

$$i\omega\rho C_p\Theta = k\nabla^2\Theta + i\omega\alpha T_0 P + Q, \tag{12}$$

$$P = c^2\varrho + \alpha\Theta\gamma\rho_0. \tag{13}$$

When solving the system (10)–(13), the following boundary conditions were used for the geometry shown in Fig. 2: $\Theta = 0$, $\mathbf{u} = 0$. The heat flow was considered as the source of the acoustic wave

$$Q = Q_0 e^{-\frac{\zeta}{\gamma}-D/2)^2+x^2}2\sigma^2,$$

where $\sigma = \frac{2}{3}r$. Figure 3 shows the distribution of Q in the cell cross-section.

Results

According to the laws of an ideal fluid hydrodynamics, an increase in the resonator cross-section in the area of the microphones relative to the initial resonators cross-section should lead to a rise of pressure on them. The longitudinal shape of the resonators was varied by changing the coefficient k, describing the maximum radius of the resonators (Fig. 2). The shape varied from r to kr. Parameter k changed from 1 to 2.4.

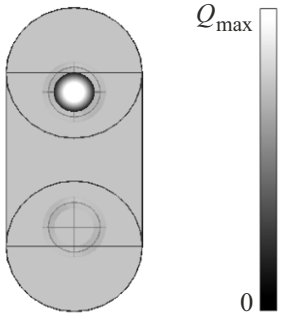

Figure 3. Distribution of the heat flow Q in the cell cross-section.

Fig. 4 shows the spatial pressure profiles in three mutually perpendicular sections of OAD for the first resonant mode at $k = 1$, at $k = 1.8$ for the first geometry, and $k = 1.6$ for the second geometry.

In each of the variants, the maximum and minimum pressures for the first resonant mode are located in the centers of the resonators.

The change in acoustic resonance frequency for the first ring mode as a function of k is shown in Fig. 5. It can be seen that there is a slight monotonous decrease in the resonant frequency. This effect may be useful when using parametric light generators, since reducing the modulation frequency of the laser pump source diminishes the thermal load on a nonlinear crystal.

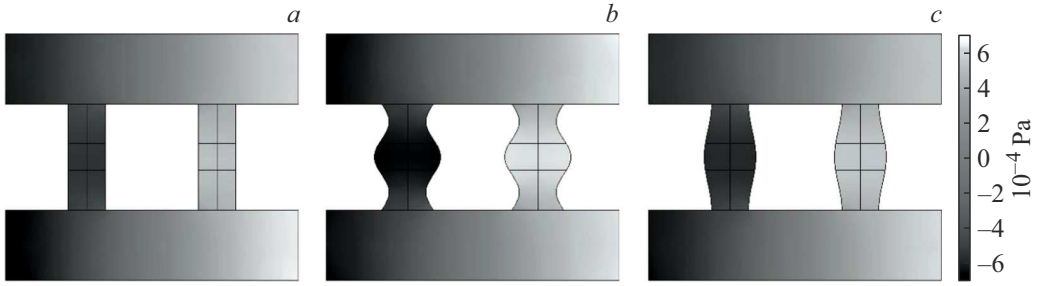

Figure 4. Pressure distribution for the first resonant mode in the horizontal section of OAD at $k = 1$ and a resonant frequency of 1255 Hz (a), at $k = 1.8$ and a resonant frequency of 1226 Hz for the first geometry (b), $k = 1.6$ and at resonant frequency of 1236 Hz for the second geometry (c).

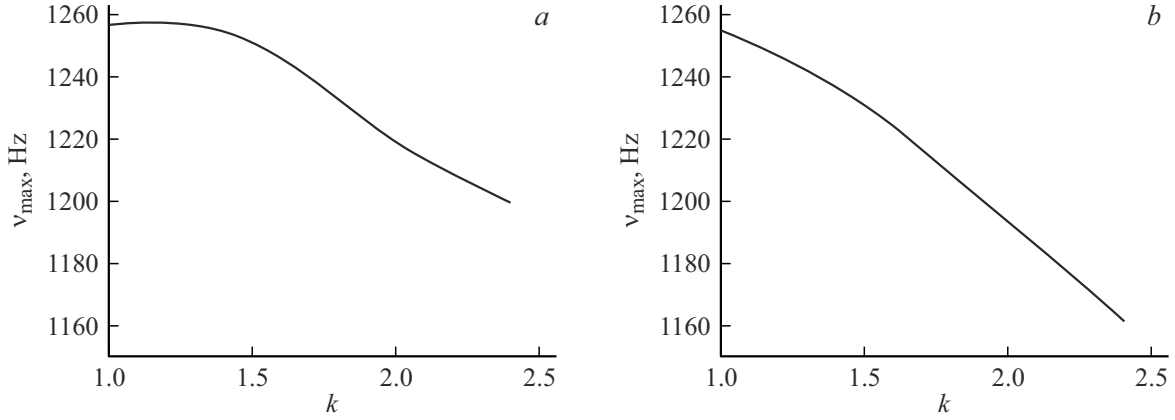

Figure 5. Resonant frequency versus parameter k for the geometry of the first (a) and (b) second types.

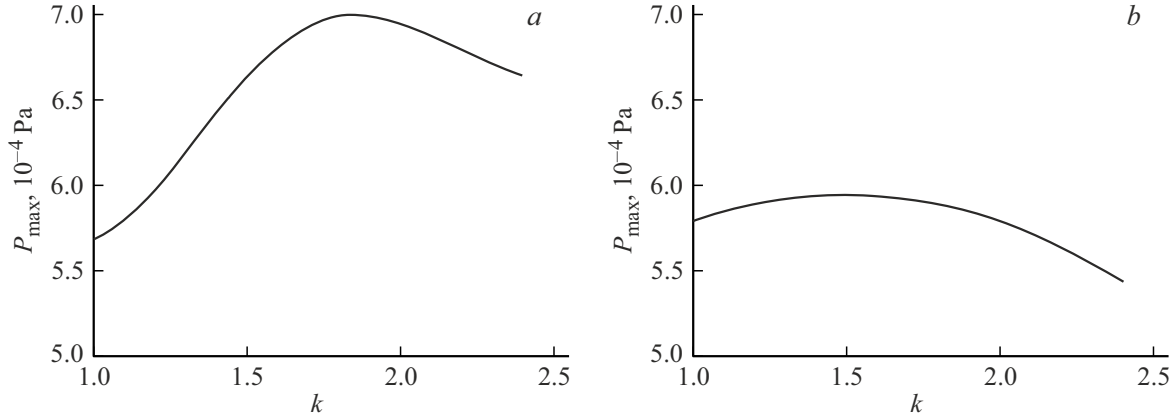

Figure 6. Maximal (amplitude) pressure in the resonators' center at resonant frequency versus k parameter for the first (a) and second (b) geometries.

The dependence of the maximum pressure amplitude P in the resonators' center at OAD resonant frequency on the parameter k for the two types of geometry, calculated using the dynamic model (10)–(13), is shown in Fig. 6. Figure 6 shows that for both types of geometry there is a value of k, at which the pressure difference in the center of neighboring resonators will be greatest, i.e. the OAD will have maximum sensitivity. In case of the first geometry, greater sensitivity can be achieved by reducing the minimum radius and increasing the maximum. It should be remembered that the minimum radius is limited by the radius of the radiation beam, and the maximum is limited by the distance between the resonators.

The dependence of Q-factor of the OAD on k for a geometric shape of the first type is shown in Fig. 7.

It is of interest to evaluate the applicability of the formula (1) to calculate the amplitude of the pressure wave

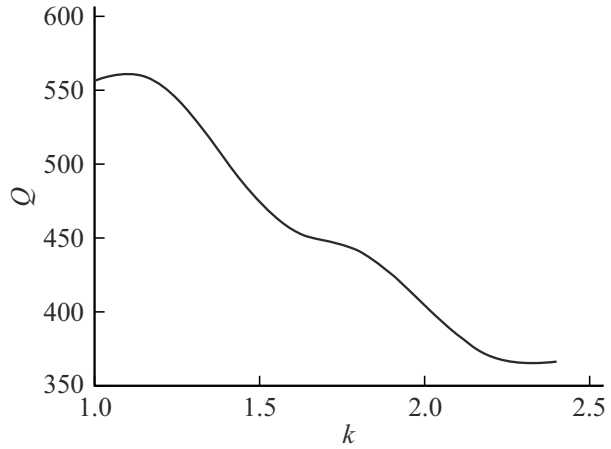

Figure 7. The dependence of Q-factor of the resonant OAD on k parameter for the first geometry.

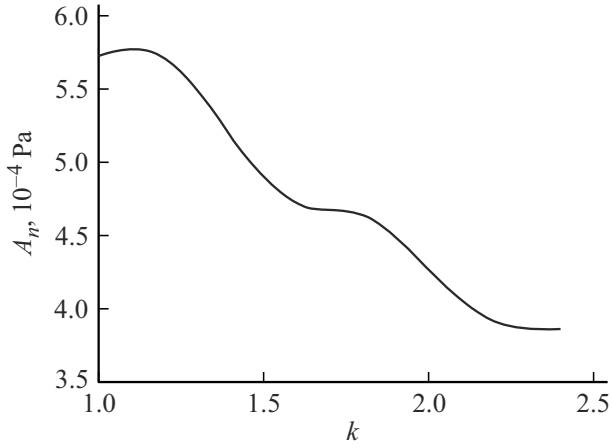

Figure 8. A_n at the resonance frequency versus parameter k for the resonant OAD with the first type of geometry.

in resonant OADs with resonators of variable cross-section. Figure 8 shows the pressure amplitude A_n calculated by formula (1), where Q-factor as a function of k was found from Figure 7, i.e. for a resonant OAD with a first type of geometry. Similarly, it was taken into account that for this geometry, the volume of the measuring cell V_{cell} also depends on this parameter (Fig. 2, *a*. Here, $n = 1$.

From Fig. 8 we see that A_n versus parameter k found by the formula (1) practically repeats the dependence of Q factor Q on parameter k (Fig. 7). However, similar dependence of the pressure amplitude in the center of the resonator (where the antinode of the standing acoustic wave is located), calculated using a dynamic model (equations (10)–(13)), is fundamentally different except for the limiting case $k = 1$ (Fig. 6). This indicates the inapplicability of the expression (1) to evaluate the sensitivity of resonant OADs with resonators of variable cross-section.

Conclusion

In this paper, an option of a resonant OAD with two cylindrical resonators of variable cross-section is proposed and analyzed. In the first option (Fig. 2, *a*) cylindrical resonators are used with their cross-section radius having two local minima which are smaller than the cross-section radius at the junction of buffer elements and resonators. In the second option, cylindrical resonators are used where the cross-section radius is minimal at the buffers-resonators junction and grows monotonously towards the center of each of the resonators. In both variants, the cross-section radius is maximal in the center of each of the resonators. Computational modeling has shown that by increasing the cross-section in the region of the standing acoustic wave antinode corresponding to the first resonant acoustic mode, it is possible to achieve higher pressure amplitude and, accordingly, higher sensitivity of the OAD. In all calculations, the minimum radius of the resonators was fixed and determined by the diameter of the laser beam.

The dependences of the pressure amplitude in the center of the resonator (where the antinode of the standing acoustic wave is located) were found using a dynamic model and using a widely used analytical formula for calculating the sensitivity of the resonant OAD. They are fundamentally different from the calculations of the dynamic model for OAD with resonators of variable cross-section. This indicates the inapplicability of the analytical expression to evaluate the sensitivity of resonant OADs with resonators of variable cross-section. The findings outlined in this study can be used to design highly sensitive optical-acoustic spectrometers.

Funding

This study was made within the state assignment of TGU, number of topic FSWM-2025-0038.

Conflict of interest

The authors declare no conflict of interest.

References

[1] A. Smolinska, A-Ch. Hauschild, R. Fijten, J.W. Dallinga, J. Baumbach, F.J. van Schooten. J. Breath Res., **8** (2), 027105 (2014). DOI: 10.1088/1752-7155/8/2/027105
[2] C. Louren co, C. Turner. Metabolites, **4** (2), 465 (2014). DOI: 10.3390/metabo4020465
[3] M.P. van der Schee, T. Paff, P. Brinkman, W. Marinus. C. van Aalderen, E.G. Haarman, P.J. Sterk. CHEST, **147** (1), 224 (2015). DOI: 10.1378/chest.14-0781
[4] L.D. Bos, P.J. Sterk, S.J. Fowler. J. Allergy Clin. Immunol., **138** (4), 970 (2016). DOI: 10.1016/j.jaci.2016.08.004
[5] A.V. Borisov, A.G. Syrkina, D.A. Kuz.min, V.V. Ryabov, A.A. Boyko, O. Zaharova, V.S. Zasedatel., Y.V. Kistenev. J. Breath Res., **15** (2), 027104 (2021). DOI: 10.1088/1752-7163/abebd4

[6] Yu.V. Kistenev, A.V. Borisov, D.A. Kuzmin, O.V. Penkova, N.Yu. Kostyukova, A.A. Karapuzikov. J. Biomed. Opt., **22** (1), 017002 (2017). DOI: 10.1117/1.JBO.22.1.017002.
[7] A.A. Boyko, A.V. Borisov, V.S. Zasedatel, V.V. Romanchuk, Yu.V. Kistenev. J. Biomed. Photonics & Engineering, **8** (4), 40301 (2022). DOI: 10.18287/JBPE22.08.040301.
[8] Y.V. Kistenev, A.V. Borisov, V.S. Zasedatel, L.V. Spirina. J. Biophotonics, **16** (9), e202300198 (2023). DOI: 10.1002/jbio.202300198
[9] C. Haisch. Measurement Science and Technology, **23** (1), 012001 (2011). DOI: 10.1088/0957-0233/23/1/012001
[10] D.C. Dumitras, D.C. Dutu, C. Matei, A.M. Magureanu, M. Petrus, C. Popa. J. Optoelectronics and Advanced Materials, **9** (12), 3655 (2007).
[11] M.A. Proskurnin, V.R. Khabibullin, L.O. Usoltseva, E.A. Vyrko, I.V. Mikheev, D.S. Volkov. UFN, **192** (3), 294 (2022) (in Russian). DOI: 10.3367/UFNe.2021.05.038976
[12] V.A. Kapitanov, A.I. Karapuzikov, Yu.N. Ponomarev, I.V. Sherstov. Resonant optical-acoustic detector and optical-acoustic laser gas analyzer. Patent of the Russian Federation No 51 746 U1, 2006.
[13] A.I. Karapuzikov, A.A. Karapuzikov, I.V. Sherstov. Optical-acoustic detector. Patent of the Russian Federation № 133 306 U1, 2013.
[14] A.A. Karapuzikov, I.V. Sherstov, D.B. Kolker, A.I. Karapuzikov, Yu.V. Kistenev, D.A. Kuzmin, M.Yu. Styrov, N.Yu. Dukhovnikova, K.G. Zenov, A.A. Boyko, M.K. Starikova, I.I. Tikhonyuk, I.B. Miroshnichenko, M.B. Miroshnichenko, Yu.V. Myakishev, V.N. Loconov. Physics Wave of Phenomena, **22** (3), 189 (2014). DOI: 10.3103/S1541308X14030054.
[15] V.N. Alferov, D.A. Vasiliev. Pribory i tekhnika eksperimenta, **1** (5), 148 (2020) (in Russian). DOI: 10.31857/S0032816220050080
[16] I.V. Sherstov, D.B. Kolker. Kvant. elektron., **50** (11), 1063 (2020) (in Russian). DOI: 10.1070/QEL17316
[17] I.V. Sherstov, V.A. Vasiliev. Infrared Physics & Technology, **119**, 103922 (2021). DOI: 10.1016/j.infrared.2021.103922
[18] S. Alahmari, X. W. Kang, M. Analytical and Bioanalytical Chemistry, **411** (17), 3777 (2019). DOI: 10.1007/s00216-019-01877-0
[19] Y.V. Kistenev, A.V. Borisov, D.A. Kuzmin, A.A. Bulanova, A.A. Boyko, N.Y. Kostyukova, A.A. Karapuzikov. Proc. SPIE 9707, Dynamics and Fluctuations in Biomedical Photonics XIII, 97070M (March 17, 2016). DOI: 10.1117/12.2214645
[20] Y.N. Ponomarev. Optika atmosfery i okeana, **8** (1), 224 (1995) (in Russian)
[21] G.K. Raspopin, D.R. Makashev, A.V. Borisov, Yu.V. Kistenev. Opt. i spektr., **130** (6), 826 (2022) (in Russian). DOI: 10.21883/OS.2022.06.52622.28-22
[22] C.M. Lee, K.V. Bychkov, V.A. Kapitanov, A.I. Karapuzikov, Y.N. Ponomarev, I.V. Sherstov, V.A. Vasiliev. Optical Engineering, **46** (6), 064302-064302-8 (2007). DOI: 10.1117/1.2748042
[23] A. Miklós, P. Hess, Z. Bozóki. Rev. Scientific Instruments, **72** (4), 1937 (2001). DOI: 10.1063/1.1353198
[24] A.L. Ulasevich, A.V. Gorelik, A.A. Kouzmouk, V.S. Starovoitov. Infrared Physics & Technology, **60**, 174 (2013). DOI: 10.1016/j.infrared.2013.04.011
[25] M. Tavakoli, M. Tavakoli, A. Tavakoli, M. Taheri, H. Saghafifar. Optics & Laser Technolog., **42** (5), 828 (2010). DOI: 10.1016/j.optlastec.2009.12.012
[26] L. Wu, T. Chen, B. Xiang, L. Xing. Appl. Sci., **14** (23), 11343 (2024). DOI: 10.3390/app142311343
[27] G. Wu, X. Wu, Z. Gong, J. Xing, Y. Fan, J. Ma, W. Peng, Q. Yu, L. Mei. Optics Express, **31** (21), 34213(2023). DOI: 10.1364/OE.502733
[28] J. M. Rey, C. Romer, M. Gianella, M.W. Sigrist. Appl. Phys. B, **100** (1), 189 (2010). DOI: 10.1007/s00340-010-3994-x.

Translated by J.Savelyeva